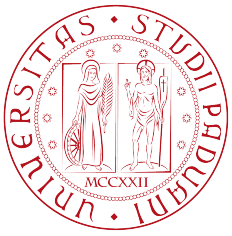

Università degli Studi di Padova

Dipartimento di Fisica e Astronomia "Galileo Galilei"
Corso di Laurea Triennale in Fisica

Tesi di Laurea

Quantum simulation of the (1+1)-dimensional $U(1)$ Lattice QED with Rydberg atoms

Relatore
Prof. Simone Montangero

Laureando
Mattia Morgavi

Anno Accademico 2019/2020

Abstract

Gauge Theories like Quantum chromodynamics (QCD) display non perturbative effects which mostly prevent their study via analytical tools. A possible approach to study and simulate these theories is the Lattice Gauge Theory formulation, i.e., a space-time discretization through a lattice. In the quantum link formulation of lattice gauge theories every field state on the link of the lattice is identified with a quantum spin state. This allows to simulate the theory via quantum systems like a chain of cold neutral atoms characterized by highly excited Rydberg states. In this thesis a brief introduction to the Lattice Quantum electrodynamics (Lattice QED) is given, focusing on its Hamiltonian formulation and on the Gauss' law constraint. An example of a Rydberg atoms quantum simulator for the quantum link formulation of a $(1 + 1)$-dimensional $U(1)$ lattice gauge QED is presented. Finally, we will numerical simulate the time-evolution of a small-scale system with exact diagonalization techniques.

Contents

Introduction

Quantum Field Theories (QFTs) are the basic tools to formalize modern fundamental physics. The known interactions (electromagnetic, weak, strong), described by the *Standard Model*, are associated to the invariance of the system under certain groups of transformations, called gauge groups. For example, *Quantum Electrodynamics* (QED) is associated to the Abelian $U(1)$ group, while strong interactions characterizing *Quantum Chromodynamics* (QCD) are associated to a non-Abelian group.

Due to the non-perturbative effects arising in the study of fundamental interactions, numerical solutions have been adopted, such as the *Lattice Gauge Theory* (LGT) formulation, which overcomes non-perturbative problems with a space-time discretization through a lattice [1], where particles and gauge fields reside on sites and bonds of the lattice respectively [2]. Here we focus on the (1+1)-dimensional $U(1)$ lattice gauge QED, which describes the interactions between fermionic electric charges and an electric field characterized by a discrete, unbounded spectrum [1]. The *Quantum Link Model* (QLM) is a formulation of gauge theories, in which every field state on the link of the lattice is identified with a quantum spin state [3]. Thus, with spin-$\frac{1}{2}$ and a finite lattice of $L+1$ sites indexed with $j = 0, \dots, L$, all the possible quantum states of the pure gauge theory span to a finite-dimensional Hilbert space $\mathcal{H}$ which dimension scales as 2^L. Hence, the system and its evolution is computationally manageable using $2^L \times 2^L$ operator matrices. Restricting the analysis to a small number of sites ($L \sim 10$) we can straightforwardly exploit exact diagonalization methods to solve the dynamics of the system. As L increase ($L \gg 10$) classical methods like *Matrix Product State* (MPS) with *tensor networks* (TNs) have been developed [4]. A *quantum simulation* is another promising way to study LGTs and quantum many-body systems dynamics. The first insight into the use of a universal quantum computer as a quantum system to simulate quantum world comes from 1982 Feynman's seminal article [5]. Using real quantum systems to simulate the dynamics of another quantum system, gives an exponential gain in terms of computational cost. The most challenging task to quantum simulate an LGT is finding a system whose Hamiltonian can be mapped to the one of the LGT [6]. Cold neutral atoms highly excited to Rydberg states are promising quantum systems to realize strongly interacting quantum matter and simulate real-time dynamics of LGTs. Here we focus on the quantum system of Rydberg atoms chain described in [7], which can be seen as a spin chain system, so the states of this system can be mapped to the ones of the QLM [6].

In chapter 1 we present a brief introduction to the Lattice QED, focusing on Hamiltonian structure and Gauss' law constraint, adapting the theory to a QLM formulation. In chapter 2 we show that the Hamiltonian of the system of Rydberg atoms can be mapped into the QLM version of the lattice QED Hamiltonian. Finally, we show that Rydberg atoms systems are an efficient way to simulate the QED on a lattice (Fig. 1). In chapter 3 we report numerical simulations of simple systems dynamics, simulating QLM and Rydberg atoms Hamiltonian using a small scale lattice and exact diagonalization technique for time evolution. We provide classical simulations of a small-scale ($L \lesssim 20$ lattice sites) system of Rydberg atoms, solving the time evolution via QuTip Python library. Results of the numerical simulation are commented and compared with results present in the literature. Finally, in chapter 4, the conclusions and future outlooks are given.

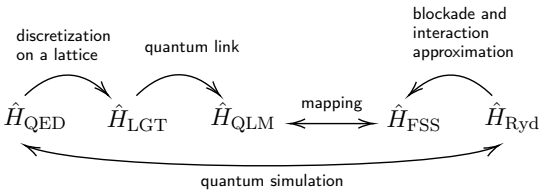

Figure 1: Scheme of the Hamiltonians introduced in chapter 1 and 2. The final aim is simulating the 1D QED Hamiltonian $\hat{H}_{\mathrm{QED}}$ with the Hamiltonian $\hat{H}_{\mathrm{Ryd}}$ of a real quantum system.

Chapter 1

The $(1+1)$-dimensional Lattice QED

In this chapter a brief overview of the Schwinger model and the lattice adaptation of the $(1+1)$-dimensional QED is given. Then, we describe the structure of the LGT version of the QED Hamiltonian and the gauge symmetry constraint for that theory (the Gauss' law). We finally introduce the spin-$\frac{1}{2}$ QLM formulation for this LGT.

1.1 $(1+1)$-dimensional QED: the Schwinger model

Julian Schwinger first investigated [8] the properties of QED in $(1+1)$-dimension with a single Dirac fermion with mass m, after named *Schwinger model*.

Denoting with σ^i the Pauli matrices, we first define the 4×4 matrices

$$\gamma^0 = \begin{pmatrix} \mathbb{0} & \mathbb{1} \\ \mathbb{1} & \mathbb{0} \end{pmatrix} , \qquad \gamma^i = \begin{pmatrix} \mathbb{0} & -\sigma^i \\ -\sigma^i & \mathbb{0} \end{pmatrix} .$$

Indicating with $\hat{\psi}$ the 4-component Dirac spinor (the matter field), and with $\hat{\overline{\psi}} = \hat{\psi}^\dagger \gamma^0$ the Dirac adjoint, the continuum Hamiltonian of the Schwinger model can be written as [11]

$$\hat{H}_{\text{QED}} \;=\; -i\gamma^1 \int \mathrm{d}x\, \hat{\overline{\psi}} \hat{D}_1 \hat{\psi} \;+\; m \int \mathrm{d}x\, \hat{\overline{\psi}} \hat{\psi} \;+\; \frac{1}{2} \int \mathrm{d}x\, \hat{\mathbf{E}}^2 \,. \tag{1.1}$$

where $\hat{D}_\mu = \partial_\mu + i\hat{A}_\mu$ is the covariant derivative and $\hat{\mathbf{E}}$ is the electric field (existence of magnetic field $\hat{\mathbf{B}}$ is not permitted in dimension $d = 1$ [11]). The first term of (1.1) is the coupling between mass and the field, the second one is the mass term of fermions while the third one is the electrostatic energy of the field.

In $(3+1)$-dimensional QED the potential energy between charged particles scales with distance as $1/r$. Differently, in $(1+1)$-dimension the dependence is linear with distance. This brings to *confinement* [1] between particles in the Schwinger model, analogous to the quarks color confinement of $(3+1)$-dimensional QCD.

Confinement in QCD means that quarks are never isolated: when a couple of quarks of a meson are distant enough, the energy of the field induces the spontaneous production of a couple of quark-antiquark pair between them. This process, called *hadronization* or *fragmentation*, reduces the distance between the particles, originating jets of particles. Fragmentation of QCD has a counterpart in the Schwinger model: the *string breaking* [1] (Fig. 1.1). A *string* is a region of 1-dimensional space between a couple of opposite charges, where the electric field is uniform. String breaking is one of the phenomena which makes the Schwinger model a toy model of more complex theories like QCD [9, 10].

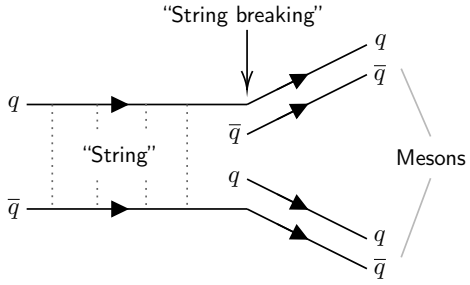

Figure 1.1: Hadronization or string breaking involves two particles with opposite charges: the distance between particles can increase until the energy of the field is enough to create a particle-antiparticle pair, reducing distance creating bound states (mesons). The string breaking phenomenon in the Schwinger model is analogous to the hadronization process in the 3-dimensional QCD.

Even j	Odd j
○ $= \emptyset$	○ $= \overline{q}$
● $= q$	● $= \emptyset$

Table 1.1: The Kogut-Susskind staggered fermions convention. This formulation allows to represent three different states (vacuum, particle and antiparticle state) in the lattice using only two states for the lattice sites. The fundamental unit of the lattice thus becomes a pair of sites.

1.2 Discretization on a lattice

In a $(1+1)$-dimensional LGT the physical space is discretized with a 1-dimensional lattice: we consider a finite set of $L+1$ equidistant points in the real line indexed with $j = 0, \ldots, L$. Matter is represented by a fermionic particles field (or *matter field*) $\hat{\psi}_j$, on each site j of the lattice. The gauge electric field $\hat{E}_{j-1,j}$ lives on the L lattice bonds defined between neighboring sites:

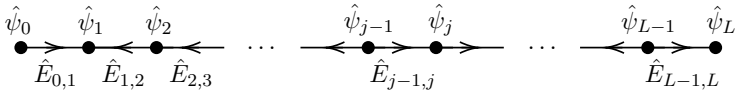

Figure 1.2: Schematic representation of a 1-dimensional lattice with fields.

The matter field operators obey the fermionic *canonical anti-commutation relations* [11]

$$\{\hat{\psi}_j, \hat{\psi}_k\} = 0 \,, \qquad \{\hat{\psi}_j^\dagger, \hat{\psi}_k\} = \delta_{j,k} \,. \tag{1.2}$$

On the other hand, the gauge field operators commute as

$$[\hat{E}_{j-1,j}, \hat{A}_{k-1,k}] = i\delta_{j,k} \,, \qquad [\hat{E}_{j-1,j}, \hat{U}_{k-1,k}] = \delta_{j,k}\hat{U}_{j-1,j} \,, \tag{1.3}$$

where $\hat{U}_{j-1,j} = e^{-i\hat{A}_{j-1,j}}$ is the parallel transporter with $\hat{A}_{j-1,j}$ the vector potential.

We impose the *open boundary condition* [6] of constant electric field outside of the lattice, so $\hat{E}_{j-1,j} = \hat{E}_{k-1,k} = \text{const.}$ for all $j, k \notin [1, L]$.

To represent matter (particles q) and antimatter (anti-particles $\overline{q}$) the *Kogut-Susskind staggered fermions* formulation is adopted [2]. Each site of the lattice has two possible states: void (○) or filled (●). Odds and even sites of the lattice are different: on even sites, a filled node is matter and unfilled node is vacuum; on odd sites a filled node is vacuum and unfilled node is anti-matter (table 1.1).

The Hamiltonian (1.1) can be adapted [11] to the discretized staggering fermions lattice counterpart

$$\hat{H}_{\text{LGT}} \;=\; -w\sum_{j=1}^{L}\left(\hat{\psi}_{j-1}^\dagger \hat{U}_{j-1,j}\hat{\psi}_j + \text{h.c.}\right) \;+\; m\sum_{j=0}^{L}(-1)^j\hat{\psi}_j^\dagger\hat{\psi}_j \;+\; J\sum_{j=1}^{L}\hat{E}_{j-1,j}^2 \,. \tag{1.4}$$

The three sum terms of Eq. (1.4) represent the discretized corresponding integral terms of Eq. (1.1).

The fundamental element of the lattice needs to represent both positive and negative charges (to ensure, among other things, the local conservation of charge). Therefore the fundamental element of the lattice is a couple of neighboring sites, so that the number of lattice sites $L+1$ has to be even, from which L is odd.

Table 1.2: In spin 1/2 QLM formulation the spectrum of electric field has two opposite values. Thus, in this formulation there are 8 possible configurations of a couple of lattice bonds, using Kogut-Susskind staggered fermions. Here are listed the 6 configurations of neighboring lattice bonds with electric field allowed by Gauss' law constraint. This constraint allows to identify all the states considering only matter or gauge fields.

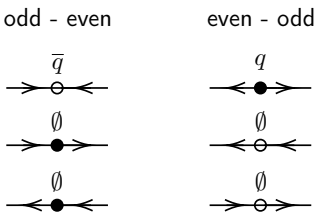

1.3 The Gauss' law constraint

Let $\mathcal{H}$ be the Hilbert space of all the possible configurations of the fields in the lattice. We define the electric field divergence operator and the charge density operator respectively as

$$(\nabla \cdot \hat{E})_j = \hat{E}_{j,j+1} - \hat{E}_{j-1,j} \ , \qquad \hat{\rho}_j = \hat{\psi}_j^\dagger \hat{\psi}_j - \frac{1-(-1)^j}{2}\hat{\mathbb{1}} \, . \tag{1.5}$$

Thus we define the gauge simmetry generator operator $\hat{G}_j$ as the difference between the electric field divergence and charge density operator:

$$\hat{G}_j \ = \ (\nabla \cdot \hat{E})_j - \hat{\rho}_j \ = \ \hat{E}_{j,j+1} - \hat{E}_{j-1,j} - \hat{\psi}_j^\dagger \hat{\psi}_j + \frac{1-(-1)^j}{2}\hat{\mathbb{1}} \, . \tag{1.6}$$

In the same way as the Gauss' law $\nabla \cdot \vec{E} = \rho$ is satisfied in classical electrodynamics, the symmetry generators allow to define the quantum counterpart $(\nabla \cdot \hat{E})_j - \hat{\rho}_j = 0$. The physical states $|\Psi\rangle \in \mathcal{H}$ are those such that

$$\hat{G}_j \, |\Psi\rangle = 0 \, . \tag{1.7}$$

The constraint of Eq. (1.7) is a $U(1)$ local gauge symmetry of the lattice.

Suppose now the spectrum of the electric field $\sigma(\hat{E}_{j-1,j})$ to be discrete with two opposite values (e.g. $1/2$, $-1/2$, as in the spin-$\frac{1}{2}$ QLM). If the Gauss' law is valid, not all the local configurations of fields are allowed in the 1-dimensional case. On table 1.2 are represented all the configurations of neighboring lattice bonds with electric and matter field allowed by Gauss' law constraint.

Let be $\mathcal{H}_G = \{|\Psi\rangle \in \mathcal{H} \mid \hat{G}_j \, |\Psi\rangle = 0\}$ the subspace of $\mathcal{H}$ of all the states which obey Eq. (1.7). If $\sigma(\hat{E}_{j-1,j}) = \{1/2, -1/2\}$ the Gauss' law constraint allows for a simplification of the space state. Let $\mathcal{H}_\psi$ and $\mathcal{H}_U$ be the state space of all the matter field and the gauge field configurations respectively. The total gauge invariant space can be written as $\mathcal{H}_G = \mathcal{H}_\psi \otimes \mathcal{H}_U$. It is straightforward to see that, imposing the open boundary condition, from a specific configuration of the electric field $\hat{E}_{j-1,j}$ is possibile to reconstruct the matter field $\hat{\psi}_j$ imposing the Gauss' law to be true [16] (and vice-versa, starting from matter field). Thus, for each state $|\Psi\rangle \in \mathcal{H}_G$ a correspondence between the fermionic and gauge states holds. This ensures a bijection $\mathcal{H}_\psi \leftrightarrow \mathcal{H}_U$ between field states, and this also allows the bijection $\mathcal{H}_U \leftrightarrow \mathcal{H}_\psi \otimes \mathcal{H}_U = \mathcal{H}_G$. Hence, imposing the Gauss' law allows to restrict the analysis of the system exclusively to one of the two fields, since the other can be derived accordingly. In our case we will consider gauge fields, since matter fields can be derived from them.

1.4 Local conservation of the gauge operator

In this section we will show that $[\hat{G}_j, \hat{H}_{\mathrm{LGT}}] = 0$, from which $\hat{G}_j$ is a local conserved quantity of the system dynamics. Consequently, if the initial state is inside $\mathcal{H}_G$, it remains inside it during time evolution (figure 1.3).

We start observing that the operators of matter field commutes with the gauge field ones, acting on different Hilbert spaces. For the same reason, two operators commutes if they acts on different sites or lattice bonds. The term $\frac{1-(-1)^j}{2}\hat{\mathbb{1}}$ of $\hat{G}_j$ commutes with any operator (is a multiple of the identity).

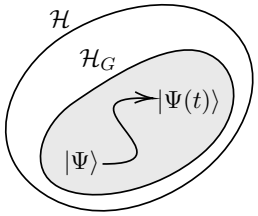

Figure 1.3: Gauge invariant dynamics with an initial state $|\Psi\rangle$ chosen inside the gauge invariant subspace $\mathcal{H}_G$: the time evolution keeps the system inside $\mathcal{H}_G$. This is guaranteed by the fact that the LGT Hamiltonian and the gauge symmetry operator commute, that is $[\hat{G}_j, \hat{H}_{\text{LGT}}] = 0$. Therefore, Gauss' law is valid $\forall t$ in the dynamics of the systems with initial state inside $\mathcal{H}_G$.

The mass term of $\hat{H}_{\text{LGT}}$ commutes with both the divergence operator of the electric field, and the occupation operator $\hat{\psi}_j^\dagger \hat{\psi}_j$, in fact $[\hat{\psi}_j^\dagger \hat{\psi}_j, \hat{\psi}_k^\dagger \hat{\psi}_k] = 0$ for each j, k. Furthermore, as $[\hat{E}_{j-1,j}, \hat{E}^2_{k-1,k}] = 0$ for each j, k we have that the electrostatic energy term commutes with the divergence term, as well as the occupation operator. Hence, the equation $[\hat{G}_j, \hat{H}_{\text{LGT}}] = 0$ is reduced to

$$[\hat{G}_j, \hat{H}_{\text{LGT}}] = \left[\hat{E}_{j,j+1} - \hat{E}_{j-1,j} - \hat{\psi}_j^\dagger \hat{\psi}_j \,,\; -w \sum_{k=1}^{L} \hat{\psi}_{k-1}^\dagger \hat{U}_{k-1,k} \hat{\psi}_k \;+ \text{h.c.}\right] = 0\,, \tag{1.8}$$

where the hermitian conjugate is written with respect to the whole summation. First of all, it is straightforward to see that given $\hat{A} = \hat{A}^\dagger$ self-adjoint and $\hat{B}$ any operator we have $[\hat{A}, \hat{B} + \text{h.c.}] = [\hat{A}, \hat{B}] - \text{h.c.}$ Therefore, if $[\hat{A}, \hat{B}] = 0$ then $[\hat{A}, \hat{B} + \text{h.c.}] = [\hat{A}, \hat{B}] - [\hat{A}, \hat{B}]^\dagger = 0 - 0 = 0$. Since the operator $\hat{E}_{j,j+1} - \hat{E}_{j-1,j} - \hat{\psi}_j^\dagger \hat{\psi}_j$ is self-adjoint (it is an observable), it follows that if the commutator of Eq. (1.8) taken without the hermitian conjugate part vanishes, then $[\hat{G}_j, \hat{H}_{\text{LGT}}] = 0$. In order to verify our hypothesis we start by, dividing by $-w$ the Eq. (1.8) we have

$$\left[\hat{E}_{j,j+1} - \hat{E}_{j-1,j} - \hat{\psi}_j^\dagger \hat{\psi}_j \,,\; \sum_{k=1}^{L} \hat{\psi}_{k-1}^\dagger \hat{U}_{k-1,k} \hat{\psi}_k\right] = 0\,. \tag{1.9}$$

We calculate separately the commutator of Eq. (1.9) for the divergence operator and the occupation one. Using the gauge commutation relation (1.3) we obtain

$$\begin{aligned}\left[\hat{E}_{j,j+1} - \hat{E}_{j-1,j}, \sum_{k=1}^{L} \left(\hat{\psi}_{k-1}^\dagger \hat{U}_{k-1,k} \hat{\psi}_k\right)\right] \;&=\; \sum_{k=1}^{L} \hat{\psi}_{k-1}^\dagger \big([\hat{E}_{j,j+1}, \hat{U}_{k-1,k}] - [\hat{E}_{j-1,j}, \hat{U}_{k-1,k}]\big) \hat{\psi}_k \\ \overset{(1.3)}{=}\; \sum_{k=1}^{L} (\hat{\psi}_{k-1}^\dagger \delta_{j+1,k} \hat{U}_{j,j+1} \hat{\psi}_k - \hat{\psi}_{k-1}^\dagger \delta_{j,k} \hat{U}_{j-1,j} \hat{\psi}_k) =\; &\hat{\psi}_j^\dagger \hat{U}_{j,j+1} \hat{\psi}_{j+1} - \hat{\psi}_{j-1}^\dagger \hat{U}_{j-1,j} \hat{\psi}_j\,.\end{aligned} \tag{1.10}$$

Now we calculate (1.8) for the operator $\hat{\psi}_j^\dagger \hat{\psi}_j$. Using the commutation-anticommutation identities $[\hat{A}\hat{B}, \hat{C}] = [\hat{A}, \hat{C}]\hat{B} + \hat{A}[\hat{B}, \hat{C}]$ and $[\hat{A}, \hat{B}\hat{C}] = \{\hat{A}, \hat{B}\}\hat{C} - \hat{B}\{\hat{A}, \hat{C}\}$, valid for any operators $\hat{A}, \hat{B}, \hat{C}$, and the anticommutation relations (1.2) it is possible to write the identity

$$\begin{aligned}[\hat{\psi}_j^\dagger \hat{\psi}_j, \hat{\psi}_{k-1}^\dagger \hat{\psi}_k] &= \hat{\psi}_j^\dagger [\hat{\psi}_j, \hat{\psi}_{k-1}^\dagger \hat{\psi}_k] + [\hat{\psi}_j^\dagger, \hat{\psi}_{k-1}^\dagger \hat{\psi}_k] \hat{\psi}_j \\ &= \hat{\psi}_j^\dagger \{\hat{\psi}_j, \hat{\psi}_{k-1}^\dagger\} \hat{\psi}_k - \hat{\psi}_j^\dagger \hat{\psi}_{k-1}^\dagger \{\hat{\psi}_j, \hat{\psi}_k\} + \{\hat{\psi}_j^\dagger, \hat{\psi}_{k-1}^\dagger\} \hat{\psi}_k \hat{\psi}_j - \hat{\psi}_{k-1}^\dagger \{\hat{\psi}_j^\dagger, \hat{\psi}_k\} \hat{\psi}_j \\ &\overset{(1.2)}{=} \hat{\psi}_j^\dagger \delta_{j,k-1} \hat{\psi}_k - \hat{\psi}_{k-1}^\dagger \delta_{j,k} \hat{\psi}_j\,.\end{aligned} \tag{1.11}$$

From the latter we obtain

$$\begin{aligned}\left[-\hat{\psi}_j^\dagger \hat{\psi}_j, \sum_{k=1}^{L} \left(\hat{\psi}_{k-1}^\dagger \hat{U}_{k-1,k} \hat{\psi}_k\right)\right] \;&=\; -\sum_{k=1}^{L} [\hat{\psi}_j^\dagger \hat{\psi}_j, \hat{\psi}_{k-1}^\dagger \hat{\psi}_k] \hat{U}_{k-1,k} = \\ =\; -\sum_{k=1}^{L} (\hat{\psi}_j^\dagger \delta_{j,k-1} \hat{\psi}_k - \hat{\psi}_{k-1}^\dagger \delta_{j,k} \hat{\psi}_j) \hat{U}_{k-1,k} =\; &-\hat{\psi}_j^\dagger \hat{U}_{j,j+1} \hat{\psi}_{j+1} + \hat{\psi}_{j-1}^\dagger \hat{U}_{j-1,j} \hat{\psi}_j\,.\end{aligned} \tag{1.12}$$

Adding Eq. (1.10) to Eq. (1.12) the terms cancels out, proving the relation of Eq. (1.9), from which it follows that $[\hat{G}_j, \hat{H}_{\text{LGT}}] = 0$.

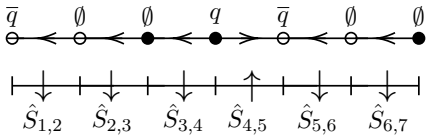

Figure 1.4: Example of two corresponding states of LGT gauge fields and QLM spin chain.

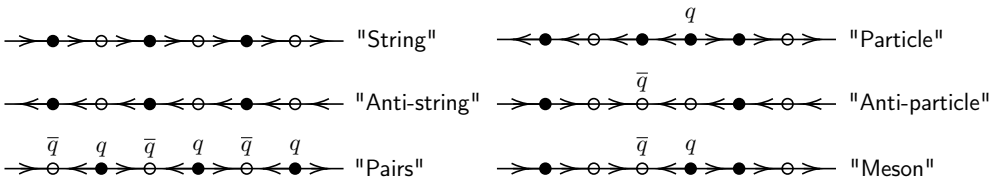

Table 1.3: The most relevant lattice QLM configurations.

1.5 Quantum Link Model formulation

In the previous section, while listing all the possible configuration of the fields on Tab. 1.2 we suppose that the space state of each gauge field lattice site operator is two-dimensional. Nonetheless, in the Schwinger model, fields can take values in a continuous spectrum. Gauge fields in Wilson's formulation of the $U(1)$ Lattice Gauge QED for example, span an infinite dimensional Hilbert space [1], due to the infinite number of degrees of freedom of the field. A formulation which instead attributes a finite number of degrees of freedom to Gauge fields is the *Quantum Link Model* (QLM) formulation [3]. The gauge field operators $\hat{E}$, $\hat{U}$, $\hat{U}^\dagger$ are mapped onto spin operators $\hat{S}^\alpha$, $\alpha = x, y, z$:

$$\hat{E}_{j-1,j} = \hat{S}^z_{j-1,j}\,, \qquad \hat{U}_{j-1,j} = \hat{S}^+_{j-1,j} = \hat{S}^x_{j-1,j} + i\hat{S}^y_{j-1,j}\,. \tag{1.13}$$

We showed that matter fields are redundant to description of LGT with Gauss' law constraint (we showed it for $S = 1/2$, but this is valid for any number of degrees of freedom): we can use only gauge fields to describe the dynamics of the system. Hence, fields are not translated in terms of real operators in the QLM with $S = 1/2$. Each configuration on the lattice field has a unique spin chain representation in the QLM, having a bijection between LGT and QLM states (Fig. 1.4).

The choices (1.13) allow to preserve the algebra (1.3) between $\hat{E}_{j-1,j}$ and $\hat{U}_{j-1,j}$, since an analogous commutation relation between spin operators holds:

$$[\hat{S}^z_{j-1,j}, \hat{S}^+_{j-1,j}] = \hat{S}^+_{j-1,j}\,. \tag{1.14}$$

However, we highlight that the operators $\hat{S}^\pm_{j-1,j}$ are no longer unitary as $\hat{U}_{j-1,j}$. It can be shown that unitarity is recovered for $S \to \infty$ [20].

We notice that if $S = 1/2$ the electrostatic energy is the same for every state, thus the third term of (1.4) is constant, in fact $J\sum_j \hat{E}^2_{j-1,j} = J\sum_j (\hat{S}^z)^2_{j-1,j} = J\sum_{j=1}^L \left(\frac{1}{2}\right)^2 \hat{\mathbb{1}} = J\,\frac{L}{4}\hat{\mathbb{1}}$. Hence, the electrostatic energy term can be neglected, obtaining the QLM Hamiltonian

$$\hat{H}_{\mathrm{QLM}} \;=\; -w\sum_{j=1}^{L}\left(\hat{\psi}^\dagger_{j-1}\hat{S}^+_{j-1,j}\hat{\psi}_j + \mathrm{h.c.}\right) \;+\; m\sum_{j=0}^{L}(-1)^j\hat{\psi}^\dagger_j\hat{\psi}_j\,. \tag{1.15}$$

Therefore, if we aim to simulate the LGT with a quantum system, the next target is finding a real system whose Hamiltonian could be set to the same form of (1.15). In the next chapter we show a particular ultra-cold atoms chain quantum system whose Hamiltonian allows this mapping.

Chapter 2

The Rydberg atoms quantum simulator

In this chapter we provide an implementation of a quantum simulator of the LGT dynamics with the QLM Hamiltonian (1.15), using a chain of L Rydberg atoms. We show how the Hamiltonian of this quantum system can be mapped to the QLM Hamiltonian of the LGT presented in the previous chapter.

2.1 Rydberg atoms chain quantum system

A cold neutral ^{87}Rb atoms array is prepared by using optical tweezers [7]. Each atom has two possible states (with quantum superpositions): a ground state $|g\rangle = |\downarrow\rangle$ $(5S_{1/2})$ and a Rydberg state $|r\rangle = |\uparrow\rangle$ $(70S_{1/2})$. Since each atom can assume two quantum states, the system is equivalent to a spin chain whose state space is the Hilbert space $\mathcal{H}_{S=1/2}^{\otimes L}$. Thus, we can use the notation of Pauli matrices $\hat{\sigma}_j^\alpha$, with $j = 1, \dots, L$ and $\alpha = x, y, z$ to represent the state of each atom. We define the occupation operator

$$\hat{n}_j = \frac{\hat{\sigma}_j^z + \hat{\mathbb{1}}}{2}\,, \tag{2.1}$$

whose expectation value is 1 if the state of the atom at position j is $|\uparrow\rangle$, 0 otherwise.

All atoms of the chain are longitudinally excited with a laser beam of Rabi frequency 2Ω and detuning δ, hence the system dynamics is governed by the Hamiltonian [7]

$$\hat{H}_{\text{Ryd}} \;=\; \Omega \sum_{j=1}^{L} \hat{\sigma}_j^x \;+\; \delta \sum_{j=1}^{L} \hat{\sigma}_j^z \;+\; \sum_{\substack{j,k=1 \\ j<k}}^{L} V_{j,k} \hat{n}_j \hat{n}_k\,, \tag{2.2}$$

where $\hbar = 1$ is set. The first term of (2.2) is the coupling between the ground state and the Rydberg state of each atom, the second one describes the local detuning term and the last one is the interaction energy between Rydberg atoms. Due to the Van der Waals interaction potential between two Rydberg atoms, $V_{j,k}$ decays with distance $R_{j,k}$ as $1/R_{j,k}^6$, so its effect to the dynamics of the system is negligible [6] if $|j - k| > 1$.

The order of magnitude of the interaction energy $V_{j,j+1}$ of neighboring atoms is larger than the Rabi frequency 2Ω [7]. Thus, when the presence of two neighboring excited Rydberg atoms occurs in the chain, the large amount of energy given by them contributes almost to all the energy of the system.

Figure 2.1: Schematical representation of the ultracold Rydberg atoms chain. We denote with small filled circles (•) the ground states, and with big void circles (∘) the highly-excited Rydberg state.

Therefore, given a system with no neighboring excited Rydberg atoms, their production is impossible during time evolution. This phenomenon is known as *Rydberg blockade effect* [6]. Assuming valid this effect, the following constraint holds:

$$\langle \Psi(t) | \, \hat{n}_j \hat{n}_{j+1} \, | \Psi(t) \rangle = 0 \quad \forall j \in \{1, \dots, L\}, \, \forall t \geq 0 \, . \tag{2.3}$$

Hereafter, we refer to $\hat{n}_j \hat{n}_{j+1}$ as *Rydberg blockade operator*.

2.2 Fendley-Sengupta-Sachdev Hamiltonian

Assuming valid the Eq. (2.3), the interaction term of Eq. (2.2) may not be considered, in fact

$$\sum_{\substack{j,k=1 \\ j<k}}^{L} V_{j,k} \hat{n}_j \hat{n}_k \;=\; \sum_{j=1}^{L-1} V_{j,j+1} \underbrace{\hat{n}_j \hat{n}_{j+1}}_{=0} \;+\; \sum_{\substack{j,k=1 \\ j<k-1}}^{L} \underbrace{V_{j,k}}_{\simeq 0} \hat{n}_j \hat{n}_k \;\simeq 0 \, . \tag{2.4}$$

where the approximation $V_{j,k} \simeq 0$ for $|j-k| > 1$ doesn't consistently affect the dynamics of the system [6]. Using the definition given in Eq. (2.1) we have $\hat{\sigma}_j^z = 2\hat{n}_j - \hat{\mathbb{1}}$, hence the second term of Eq. (2.2) can be written as

$$\delta \sum_{j=1}^{L} \hat{\sigma}_j^z \;=\; \delta \sum_{j=1}^{L} (2\hat{n}_j - \hat{\mathbb{1}}) \;=\; \left(2\delta \sum_{j=1}^{L} \hat{n}_j \right) - L\delta\hat{\mathbb{1}} \;=\; 2\delta \sum_{j=1}^{L} \hat{n}_j + \text{const.} \, , \tag{2.5}$$

where the term $-L\delta\hat{\mathbb{1}}$ is constant so it can be removed inside the Hamiltonian. With relations (2.4) and (2.5) we obtain from Eq. (2.2) the so-called *Fendley-Sengupta-Sachdev* (FSS) *Hamiltonian* [14]

$$\hat{H}_{\text{FSS}} \;=\; \Omega \sum_{j=1}^{L} \hat{\sigma}_j^x \;+\; 2\delta \sum_{j=1}^{L} \hat{n}_j \, , \tag{2.6}$$

which operates to all physical states that satisfy the constraint of Eq. (2.3).

2.3 Mapping $\hat{H}_{\text{QLM}}$ to $\hat{H}_{\text{FSS}}$

In the previous chapter we derived the QLM Hamiltonian of Eq. (1.15) from the LGT one of Eq. (1.4). Now we map the QLM Hamiltonian into the FSS (2.6), making the Rydberg atoms chain a quantum simulator of the 1-dimensional Lattice QED. In order to do this, we first find a correspondence between $\hat{S}^{\alpha}_{j-1,j}, w, m$ of the QLM Hamiltonian and $\hat{\sigma}^{\alpha}_j, \Omega, \delta$ of the atom chain system one, identifying the two sum terms of Eq. (1.15) with the two of Eq. (2.6). Secondly, we need to find a constraint to the states of the atom chain so that the Gauss' law (mapped to the quantum system) is always satisfied. We show now that the mapping is solved by the following substitutions [6]:

$$\hat{S}^x_{j-1,j} = \frac{1}{2}\hat{\sigma}^x_j \, , \qquad w = -\Omega \, , \qquad \hat{S}^{y,z}_{j-1,j} = (-1)^j \frac{1}{2}\hat{\sigma}^{y,z}_j \, , \qquad m = -\delta \, , \tag{2.7}$$

from which we obtain

$$-w \sum_{j=1}^{L} \left(\hat{\psi}^{\dagger}_{j-1} \hat{S}^{+}_{j-1,j} \hat{\psi}_j + \text{h.c.} \right) = \Omega \sum_{j=1}^{L} \hat{\sigma}^x_j \, , \qquad m \sum_{j=0}^{L} (-1)^j \hat{\psi}^{\dagger}_j \hat{\psi}_j = 2\delta \sum_{j=1}^{L} \hat{n}_j \, . \tag{2.8}$$

In section 1.3 it was seen that for each state of the invariant gauge subspace $\mathcal{H}_G$, it is possible to erase the dependence on the matter field from Hamiltonian. Hence, for the first correspondence of Eq. (2.8) the terms $\hat{\psi}_j$ are mapped into the terms:

$$\hat{\psi}^{\dagger}_{j-1} \hat{S}^{+}_{j-1,j} \hat{\psi}_j + \text{h.c.} \;\rightarrow\; \hat{S}^{+}_{j-1,j} + \text{h.c.} = \hat{S}^{+}_{j-1,j} + \hat{S}^{-}_{j-1,j} = 2\hat{S}^x_{j-1,j} = \hat{\sigma}^x_j \, . \tag{2.9}$$

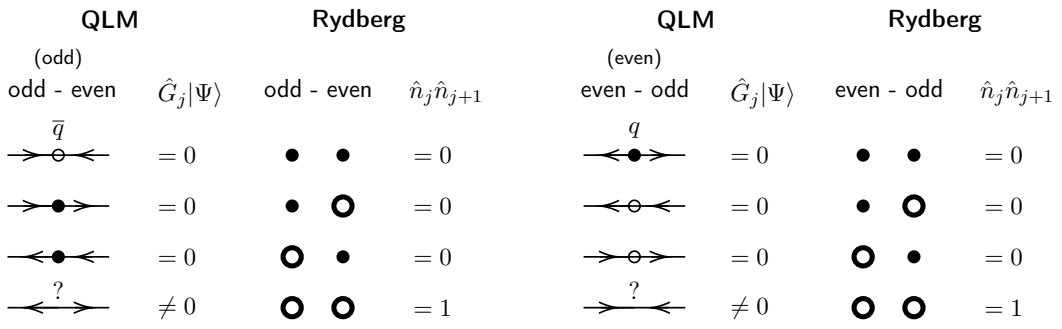

Table 2.1: Configuration correspondence between couples of Rydberg atoms and couples of spin in the QLM (represented as the respective Kogut-Susskind staggered fermion lattice site). The only configuration which doesn't respect the Gauss' law is the neighboring Rydberg atoms one, prohibited by Rydberg blockade effect.

To show a proof of the second correspondence of (2.8), we need to use the Gauss' law (1.7). The mass term can be recast as

$$m\sum_{j=0}^{L}(-1)^j\hat{\psi}_j^\dagger\hat{\psi}_j \overset{(1.5)}{=} m\sum_{j=0}^{L}(-1)^j\hat{\rho}_j \;+\; m\sum_{j=0}^{L}(-1)^j\frac{1-(-1)^j}{2}\hat{\mathbb{1}}\,. \tag{2.10}$$

The second term of (2.10) is a constant, in fact $m\sum_j(-1)^j\frac{1-(-1)^j}{2}\hat{\mathbb{1}} = \frac{m}{2}\sum_{j=0}^{L}(-1)^j\hat{\mathbb{1}} - \frac{m}{2}\sum_{j=0}^{L}\hat{\mathbb{1}} = \frac{\delta}{2}(L+1)\hat{\mathbb{1}}$, where $\sum_{j=0}^{L}(-1)^j = 0$ because L is odd. Hence, we can ignore its presence inside the Hamiltonian. We can therefore prove the second equation of (2.8) with the following steps:

$$m\sum_{j=0}^{L}(-1)^j\hat{\psi}_j^\dagger\hat{\psi}_j + \text{const.} = m\sum_{j=0}^{L}(-1)^j(\hat{E}_{j,j+1} - \hat{E}_{j-1,j}) = \tag{2.11}$$

$$\overset{(a)}{=} m(\hat{E}_{0,1} - \underbrace{\hat{E}_{-1,0}}_{\text{const.}}) + m\sum_{j=1}^{L-1}(-1)^j(\hat{E}_{j,j+1} - \hat{E}_{j-1,j}) - m(\underbrace{\hat{E}_{L,L+1}}_{\text{const.}} - \hat{E}_{L-1,L}) \tag{2.12}$$

$$\overset{(1.13)}{=} m\hat{S}^z_{0,1} + m\hat{S}^z_{L-1,L} + m\sum_{j=1}^{L-1}(-1)^j(\hat{S}^z_{j,j+1} - \hat{S}^z_{j-1,j}) \;+ \text{const.} \tag{2.13}$$

$$\overset{(2.7)}{=} \frac{\delta}{2}\hat{\sigma}^z_1 + \frac{\delta}{2}\hat{\sigma}^z_L - \delta\sum_{j=1}^{L-1}(-1)^j\left(\frac{1}{2}(-1)^{j+1}\hat{\sigma}^z_{j+1} - \frac{1}{2}(-1)^j\hat{\sigma}^z_j\right) \tag{2.14}$$

$$= \frac{\delta}{2}\hat{\sigma}^z_1 + \frac{\delta}{2}\hat{\sigma}^z_L + \delta\sum_{j=1}^{L-1}\left(\frac{1}{2}\hat{\sigma}^z_{j+1} + \frac{1}{2}\hat{\sigma}^z_j\right) \;=\; \frac{\delta}{2}\hat{\sigma}^z_1 + \frac{\delta}{2}\sum_{j=2}^{L}\hat{\sigma}^z_j + \frac{\delta}{2}\sum_{j=1}^{L-1}\hat{\sigma}^z_j + \frac{\delta}{2}\hat{\sigma}^z_L \tag{2.15}$$

$$= \delta\sum_{j=1}^{L}\hat{\sigma}^z_j \overset{(2.1)}{=} \delta\sum_{j=1}^{L}(2\hat{n}_j - \hat{\mathbb{1}}) \;=\; 2\delta\sum_{j=1}^{L}\hat{n}_j - L\delta\hat{\mathbb{1}} \;=\; 2\delta\sum_{j=1}^{L}\hat{n}_j + \text{const.}\,, \tag{2.16}$$

where in (a) open boundary conditions are applied.

We finally prove that the Rydberg blockade (2.3) is equivalent to the Gauss' law (1.7). Writing all the possible configurations of a couple of atom in the chain, and making it correspond to the relative configuration of fields in the LGT, we can easily show that for a Rydberg configuration holds $\hat{n}_j\hat{n}_{j+1} = 0$ if and only if the Gauss' law is valid for the respective LGT configuration (table 2.1). This fact is sufficient to make the dynamics of the system inside the gauge invariant space $\mathcal{H}_G$, once given an initial state at $t = 0$ which obeys the Rydberg blockade.

Chapter 3

Real-time dynamics numerical simulations

In this chapter we show the results of some classical numerical simulations related to the Rydberg atoms chain system described in the previous chapter. In particular, the vacuum state (absence of particles) and the dynamics of string breaking are analyzed varying the detuning parameter δ and the initial length l of the string. All simulations have $L = 17$ and have been performed using the exact diagonalization technique.

3.1 Notation and calculation method

The 2^L-dimensional space state $\mathcal{H}$ of the system is given by the tensor product $\bigotimes_{j=1}^{L} \mathcal{H}_j$ of the two-dimensional state spaces $\mathcal{H}_j$ of the single j-th atom system. Each space $\mathcal{H}_j$ is isomorph to the spin state space of a particle with $S = 1/2$. We use for each $\mathcal{H}_j$ the canonical orthonormal base in vector notation $|\uparrow\rangle_{(j)} = \binom{1}{0}$ and $|\downarrow\rangle_{(j)} = \binom{0}{1}$. Every operator which acts on the single space $\mathcal{H}_j$ is written in the orthonormal base, so that the corresponding spin operators $\hat{\sigma}^{\alpha}_{(j)}$, $\alpha = x, y, z$ are representable with Pauli matrices. The latter are 2×2 matrices acting on $\mathcal{H}_j$, but the respective operators of $\mathcal{H}$ are $2^L \times 2^L$ matrices which act on the single j-th atom, obtained by tensor products with identities for the remaining spaces $\mathcal{H}_{k \neq j}$:

$$\hat{\sigma}^{\alpha}_{j} = \hat{\mathbb{1}}_{(1)} \otimes \hat{\mathbb{1}}_{(2)} \otimes \ldots \hat{\mathbb{1}}_{(j-1)} \otimes \hat{\sigma}^{\alpha}_{(j)} \otimes \hat{\mathbb{1}}_{(j+1)} \otimes \cdots \otimes \hat{\mathbb{1}}_{(L-1)} \otimes \hat{\mathbb{1}}_{(L)} \,. \tag{3.1}$$

The occupation operators $\hat{n}_j$ are defined from Eq. (3.1) using the definition in Eq. (2.1).

Assigning an initial condition to the system is equivalent to set a starting sequence of excited Rydberg atoms of the chain, preparing the simulator to the initial state

$$|\Psi_0\rangle = \bigotimes_{j=1}^{L} |\alpha_j\rangle \ , \tag{3.2}$$

where $|\alpha_j\rangle \in \{|\uparrow\rangle_{(j)}, |\downarrow\rangle_{(j)}\}$ is the state vector chosen from the computational basis, assigned to the j-th atom.

The Hamiltonian we simulate is given in Eq. (2.6) with the constraint of Eq. (2.3). In order to keep the Rydberg blockade condition, the complete Hamiltonian of Eq. (2.2) is simulated: we performed that the third term of $\hat{H}_{\text{Ryd}}$ implements in fact the constraint in Eq. (2.3). However, this is not an exact equivalence, due to approximations, so we shall verify that

$$\langle \hat{n}_j \hat{n}_{j+1} \rangle_t = \langle \Psi(t) | \, \hat{n}_j \hat{n}_{j+1} \, | \Psi(t) \rangle < \epsilon \quad \forall t, \forall j = 1, \ldots, L-1 \,. \tag{3.3}$$

Therefore, the Hamiltonian of Eq. (2.2) (denoted by $\hat{H}$ for simplicity), implements the time evolution of the simulator, derivable from exact diagonalization of $\hat{H}$:

$$|\Psi(t)\rangle = e^{-i\hat{H}t} \, |\Psi_0\rangle = e^{-i\hat{H}t} \sum_{k=1}^{2^L} |\Phi_k\rangle \, \langle \Phi_k | \Psi_0 \rangle = \sum_{k=1}^{2^L} e^{-i\hat{H}t} \, |\Phi_k\rangle \, c_k \, = \sum_{k=1}^{2^L} c_k \, e^{-iE_k t} \, |\Phi_k\rangle \ , \tag{3.4}$$

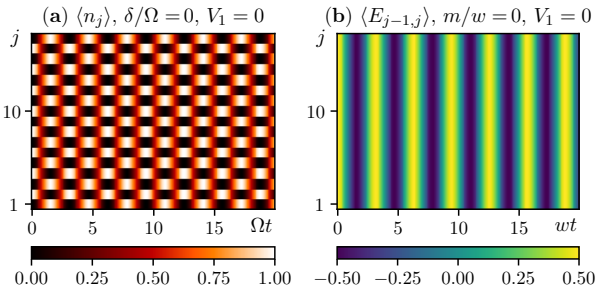

Figure 3.1: (**a**) Real-time dynamics of the Rydberg excitation density $\langle n_j \rangle$ starting from an alternating excited atoms (QLM vacuum state or string), assuming null interaction potential $V_1 = 0$. (**b**) Electric field profile $\langle E_{j-1,j} \rangle$ of the QLM translated with mapping (2.7) from dynamics of figure **a**.

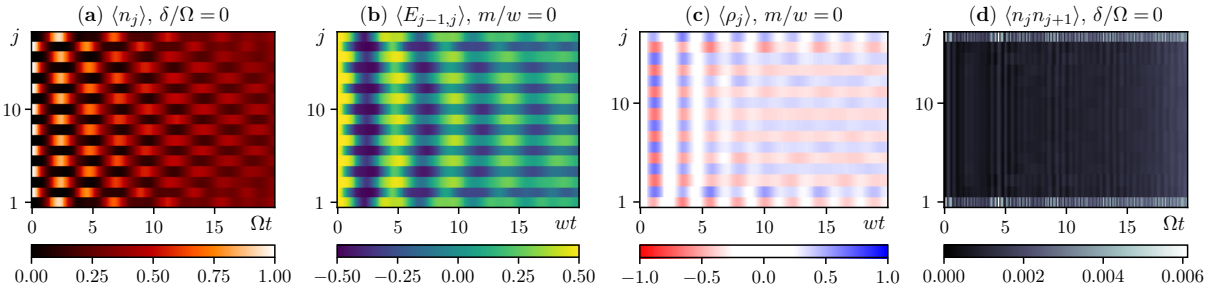

Figure 3.2: Simulation for the vacuum state with $m = -\delta = 0$ and the interaction potential. (**a**) Attenuation is visible in slow dynamics of Rydberg excitation density profile. (**b**) Time evolution of the expectation value of the QLM electric field. (**c**) Pair production is visible from the evolution of the expectation value of the charge density operator profile. (**d**) Evolution of the expectation value of the Blockade operator for each atom of the chain. Note that $\langle \hat{n}_j \hat{n}_{j+1} \rangle$ remains below the threshold $\epsilon = 10^{-2}$.

where E_k is the k-th eigenvalue of $\hat{H}$, corresponding to the eigenstate $|\Phi_k\rangle$, and $c_k = \langle \Phi_k | \Psi_0 \rangle$.

The computational time required to calculate the eigenvalues and the eigenstates scales with L as 2^L. Until $L \sim 20$ the time evolution is obtained quickly by exact diagonalization. In order to write a script which implements the quantum simulator, the open source library Quantum Toolbox in Python (QuTiP) have been used [12].

3.2 Vacuum state dynamics and Schwinger effect

Considering a chain of $L = 17$ atoms, the simulation parameters are Ω, δ, and V_1, where the latter is the proportional constant of the interaction potential inside Eq. (2.2) $V_{i,j} = k\, R_{i,j}^{-6} = V_1\ |j - i|^{-6}$. However, the three parameters have a symmetry of scale inside the Hamiltonian, therefore we can consider only the ratios δ/Ω and V_1/Ω, fixing $\Omega = 1$. Then, we will set V_1 to the realistic van der Waals potential proportional constant $V_1 = 25.6\,\Omega$ (the same introduced in [6]) letting δ/Ω (the mass m of the field) the only free parameter of the simulations.

The first dynamics we simulate is that of the vacuum, with absence of particles at $t = 0$. We start imposing $\delta = 0$ ($m = 0$). For verification purposes, the first simulation (Fig. 3.1**a**) is performed without introducing the interaction potential ($V_1 = 0$). Note that in this case the state of each atom in the chain evolves independently by oscillating with frequency $\nu = \Omega/\pi$.

By setting the interaction potential $V_1 = 25.6\,\Omega$ we obtain the dynamics shown in figure 3.2**a**. The oscillation is damped, and the electric field (Fig. 3.2**b**) alternates sign through periodic production and annihilation of particles-antiparticles pairs (Fig. 3.3). The graph of the expectation value of charge density operator $\hat{\rho}_j$ (Fig. 3.2**c**) shows alternating states of vacuum and particle-antiparticle pairs. This mechanism is the 1D analogous of the *Schwinger effect* of QED [13], or the quantum fluctuations due to electron-positron spontaneous pair production from vacuum caused by an intense electric field. Figure 3.2**d** shows that the Rydberg blockade condition is respected within a threshold

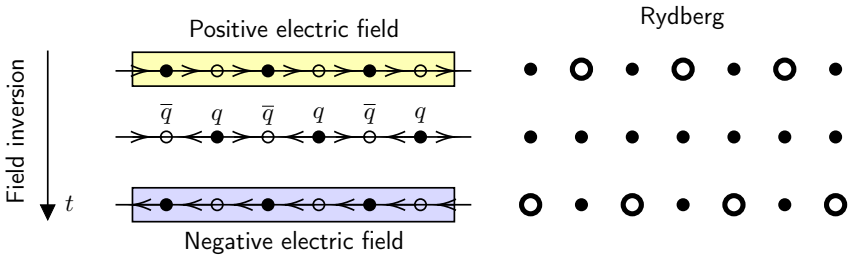

Figure 3.3: Schematization of pair production with field sign inversion in the QLM with the corresponding configuration of the quantum simulator.

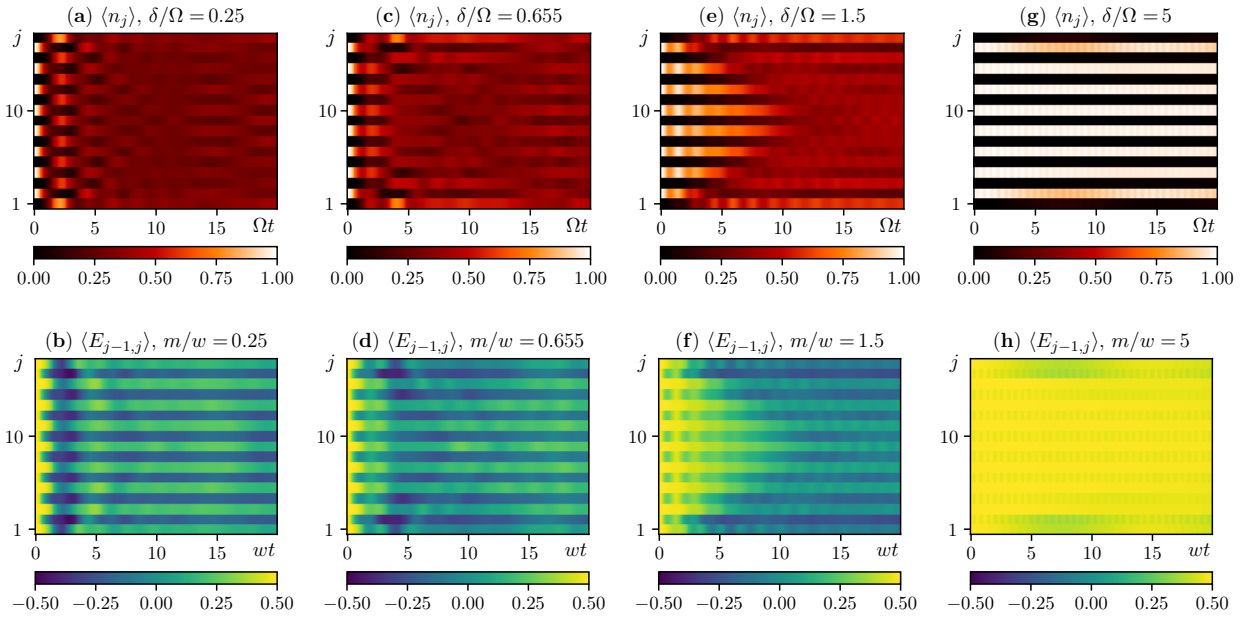

Figure 3.4: Simulation for the vacuum state of the QLM with different values of detuning parameter $\delta = -m$: **(a,b)** $|\delta| = 0.25$, **(c,d)** $|\delta| = 0.655$, **(e,f)** $|\delta| = 1.5$, **(g,h)** $|\delta| = 5$. For each simulation we controlled that the Rydberg blockade condition is respected under a threshold $\epsilon = 10^{-2}$.

$< \epsilon = 10^{-2}$.

Figure 3.4 shows the previous simulations for different values of $m > 0$, obtained by increasing the detuning δ. The particle-antiparticle creation and annihilation process is possible (Fig. 3.4**a**,**b**), until a value $\delta_c = -0.655|\Omega|$ or $m_c = 0.655|w|$ (Fig. 3.4**c**,**d**). For $|\delta| > |\delta_c|$ ($m > m_c$) the inversion of the electric field cannot be activated [6]. This is due to a spontaneous breaking of the chiral symmetry of both FSS Hamiltonian (2.6) at $\delta = \delta_c$ [14] and the QLM Hamiltonian (1.15) at $m = m_c$ [15]. Figure 3.4**e**,**f** shows the edge effects caused by the imposed open boundary conditions. In case of a very massive field, too much energy is needed to create a particle-antiparticle pair from the vacuum [11]. In the limit of $|\delta|/\Omega, m/\Omega \to \infty$ a static field is obtained (Fig. 3.4**g**,**h**).

3.3 String breaking dynamics

String breaking in the Schwinger model (Fig. 1.1) can be observed as the LGT version (Fig. 3.5). In the string breaking simulation we can modify only two parameters: the mass of the field m and the length l of the string.

Figure 3.6 simulates a real-time breaking of a string of length $l = 9$ with $m = 0$. To better visualize the string breaking, the value of the simulation with the initial vacuum condition (figure 3.2) was subtracted point by point from each graph of the second row of figure 3.6. Hence, the string breaking cleaned up from the background fluctuations, without the pair production background.

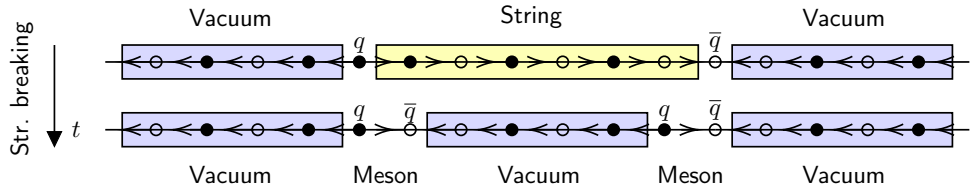

Figure 3.5: Scheme of the string braking in the QLM.

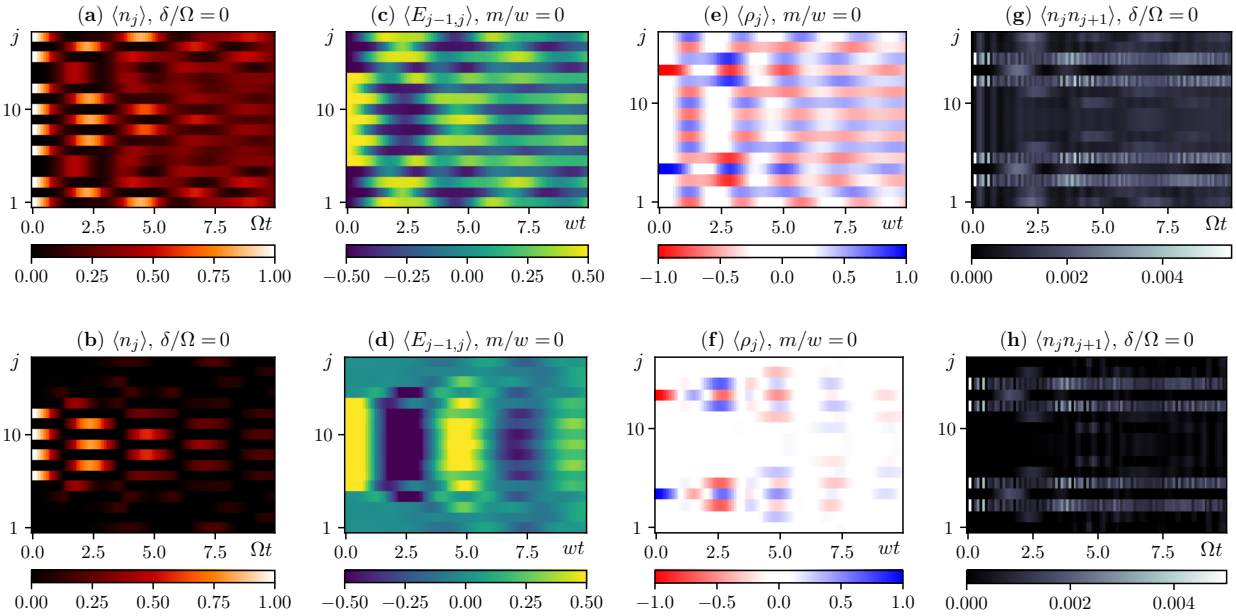

Figure 3.6: String breaking simulation with $m = 0$ and $l = 9$. (**a**) Time evolution of the expectation value of the excitation density operator of the Rydberg atoms. (**b**) Simulation of figure **a** with background noise subtraction. (**c**) Electric field expectation value profile evolution. (**d**) Background noise subtraction of figure **c**. (**e**) Charge density operator profile. (**f**) Background noise subtraction of figure **c**. We note the meson formation which breaks the string. (**g,h**) The blockade operator expectation value $\langle \hat{n}_j \hat{n}_{j+1} \rangle$ is under $\epsilon = 10^{-2}$ for each site j and every $t > 0$.

Figure 3.6**g** shows that the blockade operator expectation value remains under $\epsilon = 10^{-2}$ for each site during time evolution.

Figure 3.7 shows a string breaking simulation with $l = 9$ and different values of $m > 0$. In the second row of figure 3.7 the value of the electric field has been cleaned from the background fluctuations as for the second row of figure 3.6. We notice that the time necessary to the string to break increases with the field mass m. This is due to the fact that a greater mass of the field determines a greater energy that the electric field needs to create a pair of particles to break the string. In fact, in case of $m = 0$ field (Fig. 3.6) the string breaks almost immediatly. On the contrary, in the infinite mass limit ($|\delta| \to \infty$) the string cannot be broken (Fig. 3.7**h**).

As anticipated, the other relevant parameter in the string breaking process is the initial distance between the two particles, i.e. the initial length l of the string. Figure 3.8 shows four string breaking simulations in which $\delta = \delta_c$ is fixed while l assumes different values. Also in this figure the background noise has been cleaned up for the graphs in the second row. In this case the breaking time of the string is constant and does not depend on the string length l, even with $l = 1$ (the case of a single meson, Fig. 3.8**g,h**). Therefore the string breaking time depends only on the mass of the field.

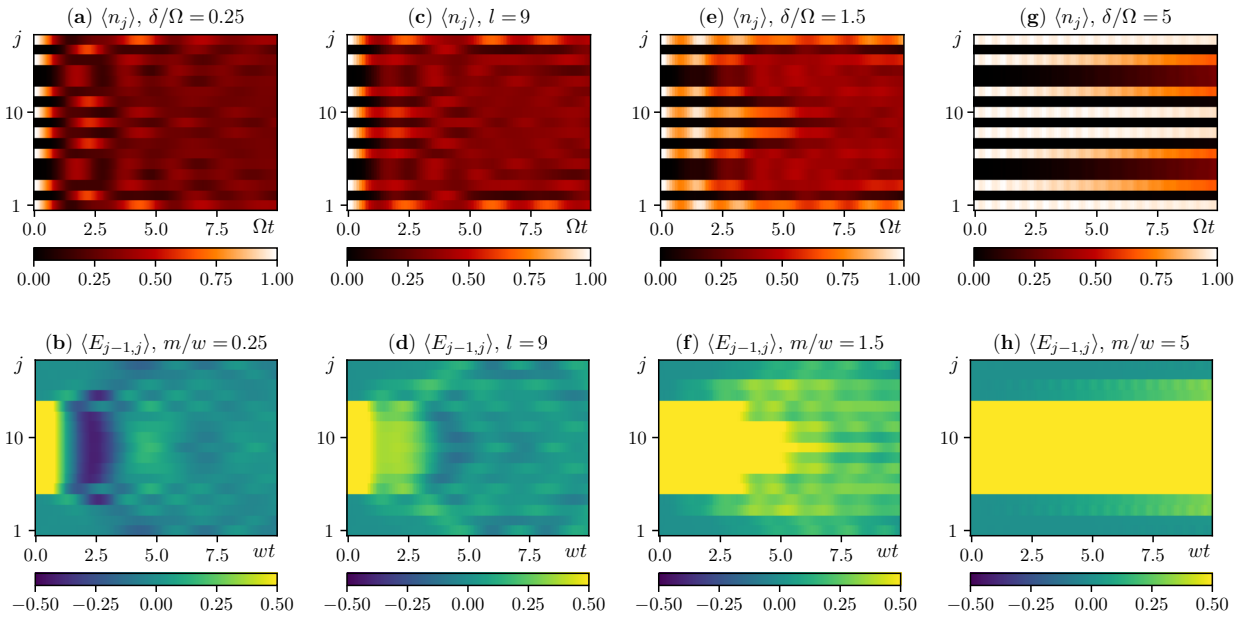

Figure 3.7: String breaking simulation with $l = 9$ and different values of m: (**a**,**b**) $|\delta| = 0.25$, (**c**,**d**) $|\delta| = 0.655$, (**e**,**f**) $|\delta| = 1.5$, (**g**,**h**) $|\delta| = 5$. In the first row, time evolution of the expectation value of the excitation density operator of the Rydberg atoms. In the second row, electric field expectation value profile evolution with noise subtraction. For each simulation we controlled that the Rydberg blockade condition is respected under a threshold $\epsilon = 10^{-2}$.

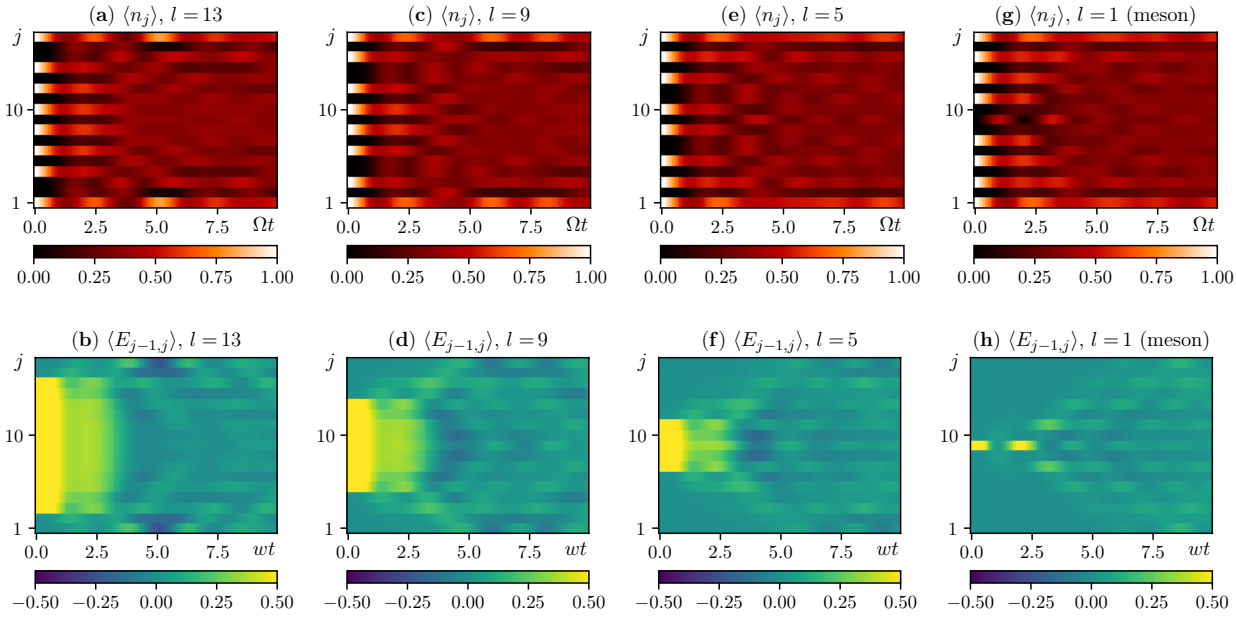

Figure 3.8: String breaking simulation with $\delta = \delta_c$ and different values of l: (**a**,**b**) $l = 13$, (**c**,**d**) $l = 9$, (**e**,**f**) $l = 5$, (**g**,**h**) $l = 1$ (meson). In the first row, time evolution of the expectation value of the excitation density operator of the Rydberg atoms. In the second row, electric field expectation value profile evolution with noise subtraction. For each simulation we controlled that the Rydberg blockade condition is respected under a threshold $\epsilon = 10^{-2}$.

Chapter 4

Conclusions and Outlook

In this thesis we presented a quantum simulator able to reproduce an Abelian Lattice Gauge Theory. We have shown how the space and the Hamiltonian of the Schwinger model of 1-dimensional QED can be discretized in an LGT. In particular, the model we used for the LGT is the spin-$\frac{1}{2}$ QLM, which by imposing the Gauss' law constraints allows to reduce the lattice gauge theory dynamics to that of a spin chain.

In order to quantum simulate this theory we have considered a physical system made up by a Rydberg atoms chain, whose Hilbert state space is equivalent to that of a spin-$\frac{1}{2}$ chain if the nearest-neighbors atoms of the chain are subject to the Rydberg-blockade mechanism. In particular, it has been shown the existence of a mapping between the local gauge invariant states of the QLM and a set of states among those of the atoms chain: this mapping matches the Hamiltonian of the QLM with the physics Hamiltonian of the Rydberg system of atoms. This fact makes the Rydberg atoms chain a quantum simulator of lattice QED.

To verify the robustness of the theoretical mapping, some classical numerical simulations of small scale Rydberg quantum simulator ($L = 17$) have been implemented with the open source Python library QuTiP. In particular, we focused on the dynamics of the bare vacuum state and on that of a string. In the last case, in particular, we studied the string breaking dynamics for different values of the mass m (varying the detuning parameter δ) and the initial length l of the string. From the simulations we observe that the breaking time of a string depends only on the mass m of the field and not on its length l. Although these simulations do not allow to reach very large lattice dimensions, they are compatible with the results obtained in the literature, as with [6, 16].

Some possible directions originating from this work, partially already considered in very recent works, are:

- Test the quantum simulator using a real Rydberg atom system, e.g. the system of [7]. In this way it will be possible to verify the results obtained with classical simulations. The main goal remains that of being able to simulate a large scale lattice ($L \gg 20$) without an exponential computational cost as for the classical simulators.

- Implement tensor network methods (TNs) with Matrix Product State representation (MPS) to classically simulate a large scale quantum simulator ($L \gg 20$) [17]. In fact, with large scale systems, it is no longer possible to solve the dynamics using exact diagonalization techniques.

- Study other models and quantum systems which can extend the lattice gauge theory to multi-dimensional ($d > 1$) quantum field theories [18, 19]. Once extended to dimension $d = 3$, it can be foreseen to quantum simulate events of interest in high energy physics, such as particle scattering or color confinement, and eventually studying non-perturbative theories like QCD.

Bibliography

[1] K. G. Wilson: *Confinement of Quarks*. Phys. Rev. D **10**, 2445 (1974). DOI: https://doi.org/10.1103/PhysRevD.10.2445.

[2] J. Kogut and L. Susskind: *Hamiltonian formulation of Wilson's lattice gauge theories*. Phys. Rev. D **11**, 395 (1975). DOI: https://doi.org/10.1103/PhysRevD.11.395.

[3] S. Chandrasekharan, U. J. Wiese: *Quantum Link Models: A Discrete Approach to Gauge Theories*. Nucl. Phys. B **492**, 455-474 (1997). DOI: https://doi.org/10.1016/S0550-3213(97)80041-7. arXiv:hep-lat/9609042. https://arxiv.org/abs/hep-lat/9609042.

[4] M. Dalmonte, S. Montangero: *Lattice gauge theories simulations in the quantum information era*. Contemp. Phys. **57**, 388 (2016). DOI: https://doi.org/10.1080/00107514.2016.1151199 arXiv:1602.03776. https://arxiv.org/abs/1602.03776.

[5] R. P. Feynman: *Simulating physics with computers*. Int. J. Theor. Phys. **21**, 467–488 (1982). DOI: https://doi.org/10.1007/BF02650179.

[6] F. M. Surace, P. P. Mazza, G. Giudici, A. Lerose, A. Gambassi, M. Dalmonte: *Lattice gauge theories and string dynamics in Rydberg atom quantum simulators*. arXiv:1902.09551 (2019). https://arxiv.org/abs/1902.09551.

[7] H. Bernien, S. Schwartz, A. Keesling, H. Levine, A. Omran, H. Pichler, S. Choi, A. S. Zibrov, M. Endres, M. Greiner, et al.: *Probing many-body dynamics on a 51-atom quantum simulator*. Nature **551**, 579–584 (2017). DOI: 10.1038/nature24622. arXiv:1707.04344. https://arxiv.org/abs/1707.04344.

[8] J. Schwinger: *Gauge Invariance and Mass. II*. Phys. Rev. **128**, 2425 (1962). DOI: https://doi.org/10.1103/PhysRev.128.2425.

[9] J. Schwinger: *The Theory of Quantized Fields I*. Phys. Rev. **82**, 914 (1951). DOI: https://doi.org/10.1103/PhysRev.82.914.

[10] J. Schwinger: *The Theory of Quantized Fields II*. Phys. Rev. **91**, 713 (1953). DOI: https://doi.org/10.1103/PhysRev.91.713.

[11] G. Magnifico: *Quantum Simulation of* $(1+1)D$ *QED via a* Z_n *Lattice Gauge Theory*. Alma Mater Studiorum, Università di Bologna. Scuola di Scienze, Tesi di Laurea Magistrale in Fisica (a.a. 2014/2015).

[12] P.D. Nation, J.R. Johansson, A.J.G. Pitchford, C. Granade, et al.: *QuTiP: Quantum Toolbox in Python, Release 4.4.0* (2019). http://qutip.org/downloads/4.4.0/qutip-doc-4.4.pdf.

[13] J. Schwinger: *On Gauge Invariance and Vacuum Polarization*. Phys. Rev. **82**, 664–679 (1951). DOI: 10.1103/PhysRev.82.664.

[14] P. Fendley, K. Sengupta, S. Sachdev: *Competing density-wave orders in a one-dimensional hard-boson model*. Phys. Rev. B **69**, 075106 (2004). DOI: https://doi.org/10.1103/PhysRevB.69.075106.

[15] E. Rico, T. Pichler, M. Dalmonte, P. Zoller, S. Montangero: *Tensor Networks for Lattice Gauge Theories and Atomic Quantum Simulation*. Phys. Rev. Lett. **112**, 201601 (2014). DOI: https://doi.org/10.1103/PhysRevLett.112.201601.

[16] S. Notarnicola, M. Collura, S. Montangero: *Real-time-dynamics quantum simulation of (1+1)-D lattice QED with Rydberg atoms*. Phys. Rev. Research **2**, 013288 (2019). DOI: https://doi.org/10.1103/PhysRevResearch.2.013288. arXiv: 1907.12579v2. https://arxiv.org/abs/1907.12579.

[17] T. Pichler, M. Dalmonte, E. Rico, P. Zoller, S. Montangero: *Real-Time Dynamics in $U(1)$ Lattice Gauge Theories with Tensor Networks*. Phys. Rev. X **6**, 011023 (2016). DOI: https://doi.org/10.1103/PhysRevX.6.011023.

[18] T. Felser, P. Silvi, M. Collura, S. Montangero: *Two-dimensional quantum-link lattice Quantum Electrodynamics at finite density*. arXiv:1911.09693 (2019). https://arxiv.org/abs/1911.09693.

[19] A.Celi, B. Vermersch, O. Viyuela, H. Pichler, M.D. Lukin, P. Zoller: *Emerging 2D Gauge theories in Rydberg configurable arrays*. arXiv:1907.03311 (2019). https://arxiv.org/abs/1907.03311.

[20] Uwe-Jens Wiese: *Towards Quantum Simulating QCD*. arXiv:1409.7414 (2014). https://arxiv.org/abs/1409.7414.